Identification of amino acid metabolism-related genes as diagnostic and prognostic biomarkers in sepsis through machine learning

YE WEN*, QIAN LIU* and WEI XU

Department of Emergency, Xianning Central Hospital, The First Affiliated Hospital of Hubei University of Science and Technology, Xianning, Hubei 437199, P.R. China

Received January 24, 2024; Accepted August 14, 2024

DOI: 10.3892/etm.2024.12786

Abstract. Previous research has highlighted the critical role of amino acid metabolism (AAM) in the pathophysiology of sepsis. The present study aimed to explore the potential diagnostic and prognostic value of AAM-related genes (AAMGs) in sepsis, as well as their underlying molecular mechanisms. Gene expression profiles from the Gene Expression Omnibus (GSE65682, GSE185263 and GSE154918 datasets) were analyzed. Based on weighted gene co-expression network analysis and machine learning algorithms, hub AAMGs were identified in the GSE65682 database. Subsequently, hub AAMGs were evaluated for their expression levels and diagnostic and prognostic significance in sepsis, as well as their interactions with regulatory pathways and role in immune cell infiltration. Additionally, trends in AAMG expression were validated using clinical samples, and their functions in sepsis were confirmed through an *in vitro* model. In total, four AAMGs were identified, two of which, methionine synthase (*MTR*) and methionine-R-isomerase 1 (*MRI1*), demonstrated significant differential expression in the GSE65682, GSE185263 and GSE154918 datasets, which was further validated using clinical samples. A diagnostic nomogram based on *MTR* and *MRI1* expression demonstrated strong diagnostic effectiveness across the three aforementioned databases. Moreover, the expression of both genes were negatively correlated with sepsis prognosis and showed stratified prognostic capabilities. Newly identified pathways included *KRAS* and *IL-2/STAT5* signaling. *MTR* and *MRI1* negatively correlated with the infiltration of inflammatory cells, such as M1 macrophages and neutrophils, and positively correlated with anti-inflammatory cells, such as $CD8^+$ T and dendritic cells. *In vitro* experiments further demonstrated that overexpression of *MTR* could mitigate the inhibition of cloning and proliferation induced by LPS and ATP in RAW 264.7 cells. These findings highlighted the potential of *MTR* and *MRI1* as biomarkers for diagnosing and prognosticating sepsis, potentially acting through the regulation of methionine in the pathophysiology of this disease. The present study provided new insights into the role of AAM in the mechanisms underlying sepsis and in the potential development of future targeted therapies.

Introduction

Sepsis, a severe medical condition typically triggered by a bacterial infection, presents with symptoms such as elevated fever, hypotension and tachycardia (1). Despite advances in medical treatments, sepsis continues to pose a significant public health challenge, with a morbidity rate of 535/100,000 individuals/year and mortality rates ranging from 25-30% (2). Therefore, it is essential to thoroughly investigate the molecular and cellular mechanisms underlying sepsis (3). Such studies are crucial for enhancing the current understanding of its pathogenesis and developing more effective treatment strategies.

Amino acid metabolism (AAM) serves a crucial role in protein synthesis and various metabolic pathways, thus being essential for understanding disease mechanisms and developing new therapies. For instance, it has been shown that mutations in glutamate metabolism-related genes can lead to metabolic disorders that severely impact liver function in certain liver diseases (4). Additionally, AAM is associated with tumor growth and invasion in certain cancer types (5). Similarly, AAM is involved in the progression of sepsis. For example, circulating N-lactoyl amino acids and N-formylmethionine can predict mortality in patients with septic shock, and glutamine helps to maintain energy metabolism and alleviate liver injury in burn-related sepsis (6,7). Consequently, a number of studies have explored the role of AAM-related genes (AAMGs) in various diseases. For

Correspondence to: Dr Wei Xu, Department of Emergency, Xianning Central Hospital, The First Affiliated Hospital of Hubei University of Science and Technology, 228 Jingui Road, Xianan, Xianning, Hubei 437199, P.R. China
E-mail: xwqsct@163.com

*Contributed equally

Key words: amino acid metabolism, methionine synthase, methionine-R-isomerase 1, sepsis, outcome prediction, disease markers, inflammation

instance, one study analyzed five AAMGs and found them to be potential biomarkers for predicting the prognosis and efficacy of immunotherapy in colorectal cancer (8). Similar research has been conducted in certain inflammatory diseases, such as identifying glutamine metabolism-related genes as diagnostic markers for diabetic foot ulcers (9). However, such studies are less common for sepsis. It is noteworthy that traditional bioinformatics methods often utilize approaches such as differential expression analysis and protein-protein interaction networks to identify hub genes (10,11). In contrast to these traditional bioinformatics methods, machine learning algorithms, despite their lower interpretability, offer improved performance, the ability to handle large-scale data and the automatic extraction of complex patterns, making them widely applicable in clinical research (12). In machine learning, the least absolute shrinkage and selection operator (LASSO) algorithm is used for feature selection, employing L1 regularization to reduce non-significant features and to enhance model interpretability and predictive performance (13). Support vector machine-recursive feature elimination (SVM-RFE) recursively selects important features to optimize feature selection for classification tasks, thereby improving classification accuracy (14). Random forests (RFs) are used for feature importance evaluation and classification, providing feature importance rankings and achieving efficient classification (15). The use of these machine learning algorithms, either individually or in combination, has yielded promising results in studies on various diseases, identifying biomarkers with high diagnostic and prognostic value, such as in sepsis (16,17). However, to the best of our knowledge, the application of these three machine learning methods in combination to investigate the role of AAMGs in sepsis remains to be investigated.

The present study, by using machine learning algorithms, identified methionine synthase (*MTR*) and methionine-R-isomerase 1 (*MRI1*) as hub AAMGs with significant diagnostic and prognostic potential in sepsis. The expression levels of these genes in patients with sepsis was validated using clinical samples from Xianning Central Hospital (Hubei, China). Additionally, the preliminary roles of *MTR* were investigated through an *in vitro* sepsis model, which demonstrated the crucial function of *MTR* in the disease's pathophysiology. The present study highlighted the importance of AAMGs in understanding the pathophysiology of sepsis and could potentially be used in the future for the development of novel targeted therapeutic interventions.

Materials and methods

Data acquisition and clinical samples. The present study utilized three datasets from the Gene Expression Omnibus (GEO) database (www.ncbi.nlm.nih.gov/geo) containing mRNA transcriptome sequencing of peripheral blood from patients with sepsis. The datasets used were GSE65682, which included samples from 760 sepsis patients and 42 healthy controls; GSE154918, comprising 40 healthy and 20 sepsis samples; and GSE185263, which consisted of 44 healthy and 26 sepsis samples. For the GSE65682 dataset, patients lacking survival data were excluded, which resulted in 479 sepsis samples with complete survival information for survival analysis. The preprocessing of the three datasets included averaging the expression values of the same gene and removing values ≤0. Principal component analysis (PCA) was conducted to confirm the differences between the sepsis and healthy groups and to demonstrate the heterogeneity among the three datasets. PCA was performed using the plot PCA function in R (http://www.bioconductor.org/) and visualized using the ggplot2 package (version 3.42) (https://cran.r-project.org/web/packages/ggplot2/index.html). Furthermore, 448 AAMGs were identified based on previous literature (8).

Table I. General clinical information of sepsis and healthy control groups.

Patient characteristic	Patients with sepsis	Healthy controls	P-value
Age, years (mean ± SD)	61.2±5.4	62.8±5.9	0.67
Male, n	4	2	0.52
Female, n	1	3	0.52

In the present study, whole blood samples were collected from five patients with sepsis who were admitted to the Department of Emergency and Intensive Care Unit of Xianning Central Hospital (Hubei, China) from March to April 2024 were selected (Table I). Inclusion criteria were as follows: i) Age, ≥18 years; ii) a definitive infection source or positive bacterial culture; and iii) compliance with sepsis criteria (18). Exclusion criteria were as follows: i) Hospitalization for <24 h; and ii) presence of malignant tumors, coronary heart disease, acute coronary syndrome, myocardial infarction, cardiogenic shock, major surgery or significant trauma. The healthy control group consisted of five individuals undergoing routine health examinations at the same hospital during aforementioned time period. The entire workflow was illustrated in Fig. 1.

Weighted gene co-expression network analysis (WGCNA) and differentially expressed genes analysis. The GSE65682 dataset was employed to identify critical AAMGs in sepsis. Initially, a co-expression network was constructed using the 'WGCNA' package (version 1.69) (19) to perform WGCNA. A total of 11,205 genes were categorized into 12 modules, with the module exhibiting the highest correlation with sepsis being selected for further analysis. Subsequently, the 'limma' package (version 3.52.1) (20) was used to obtain the differentially expressed AAMGs between sepsis and healthy samples, applying the criteria of log2 |fold change| (logFC) >1 and adjusted P<0.05. Finally, the AAMGs were acquired from the intersections of the module most highly correlated with sepsis and the genes that were significantly differentially expressed between sepsis and normal samples, and they were selected through machine learning techniques, specifically using the LASSO, SVM-RFE and RF algorithm, for detailed investigation.

Biological analysis. Gene Ontology (GO), Kyoto Encyclopedia of Genes and Genomes (KEGG) and Disease Ontology (DO) analyses were performed to elucidate the biological functions of the key AAMG. These analyses were conducted using

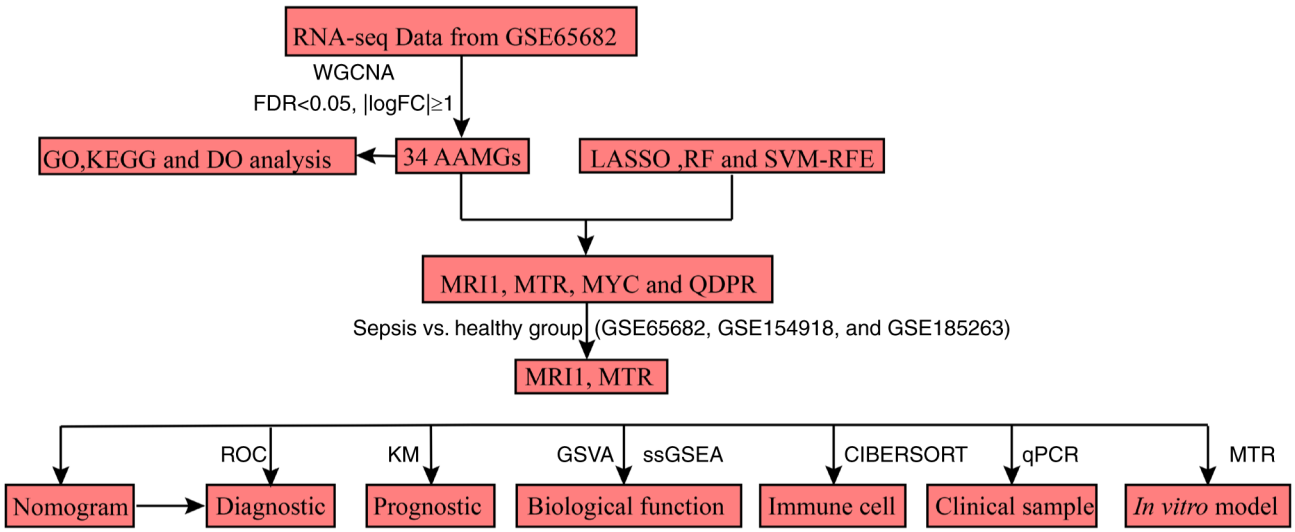

Figure 1. Flow chart of the present study. RNA-seq, RNA sequencing; WGCNA, weighted gene co-expression network analysis; FDR, false discovery rate; FC, fold-change; GO, Gene Ontology; KEGG, Kyoto Encyclopedia of Genes and Genomes; DO, Disease Ontology; AAMG, amino acid metabolism-related genes; LASSO, least absolute shrinkage and selection operator; RF, random forest; SVM-RFE, support vector machine-recursive feature elimination; MRI1, methionine-R-isomerase 1; MTR, methionine synthase; MYC, MYC proto-oncogene; QDPR, quinoid dihydropteridine reductase; ROC, receiver operating characteristic; KM, Kaplan-Meier; GSVA, gene set variation analysis; ssGSEA, single-sample gene set enrichment analysis; RT-qPCR, reverse transcription-quantitative PCR.

the 'clusterProfiler' (version 4.4.1) (21) and 'DOSE' (version 3.22.0) (22) packages. Additionally, single-sample Gene Set Enrichment Analysis (ssGSEA) analysis was performed on the GSE65682 dataset to identify different pathway activations between sepsis and healthy samples using the 'GSVA' package (version 4.4.1) (23).

Machine learning algorithm to identify hub AAMGs. To identify AAMGs most closely associated with sepsis, a robust feature selection procedure was employed: First, L1 regularization via LASSO analysis was performed using the 'glmnet' package (version 4.1-4) (24). The optimal penalty parameter (λ) was determined based on 10-fold cross-validation with the lowest deviance probability. Genes with non-zero coefficients were retained to reduce data dimensionality, ultimately obtaining a model with fewer variables (25). The present study calculated LASSO-Cox coefficients using a Lasso regression model to select key AAMGs in sepsis. Next, the SVM-RFE algorithm was used, which is a backward elimination method designed to optimize classifier performance by selecting the best subset of features. SVM-RFE analysis was conducted using the 'e1071' package (version 1.7-4) (26) to determine the most relevant AAMGs associated with sepsis. Subsequently, the RF algorithm was used for feature importance evaluation and classification. The 'randomForest' package (version 4.7-1.1) (27) was used to identify AAMGs with a relative importance >0.5, and these AAMGs were subsequently ranked by importance from highest to lowest for further analysis. The RF algorithm was suitable for both classification and regression tasks, which was ideal for the present analysis (28). By integrating results from LASSO, SVM-RFE and RF analyses, key AAMGs in sepsis were identified. These candidate AAMGs were validated in the GSE65682, GSE154918 and GSE185263 cohorts, assessing their expression levels between sepsis and healthy samples. Genes with inconsistent expression levels across the GSE65682, GSE154918 and GSE185263 datasets were excluded. Ultimately, through the methods described as aforementioned, two critical AAMGs were identified: *MTR* and *MRI1*.

Assessment of the diagnostic and prognostic value of AAMGs in sepsis. The diagnostic value of *MTR* and *MRI1* in sepsis was assessed in the GSE65682, GSE154918 and GSE185263 cohorts. Furthermore, based on the expression levels of *MTR* and *MRI1*, a nomogram was also built using the 'rms' package (version 6.3-0) (https://CRAN.R-project.org/package=rms) for these cohorts. The effectiveness of the nomogram was evaluated using the area under the curve (AUC) derived from the receiver operating characteristic curve. The prognostic value of *MTR* and *MRI1* for sepsis was demonstrated in the GSE65682 dataset, where the samples were divided into two datasets using random sampling (3:7) for bootstrap-based internal validation, a method used to assess the reliability and stability of the results within the same dataset. Moreover, the combined prognostic value of *MTR* and *MRI1* was evaluated using the same validation approaches. Kaplan-Meier survival curves were generated to illustrate prognosis using the 'survival' (version 3.5-5) (https://CRAN.R-project.org/package=survival) and 'survminer' packages (version 0.4-9) (https://CRAN.R-project.org/package=survminer).

Cell culture and in vitro sepsis model establishment. Macrophages act as the first line of host immune defense during sepsis, responding rapidly to injury (29). The balance between pro-inflammatory and anti-inflammatory cytokines that macrophages produce influences the inflammatory response and patient outcomes in sepsis (30). Therefore, macrophages are widely used in *in vitro* studies of sepsis. Commonly used cell lines include RAW 264.7 and THP-1. RAW 264.7 cells can be used directly without differentiation, providing simplicity and stability for experimental use, and are widely adopted in

many studies (31-33). Although THP-1 cells are more relevant in simulating the human response to sepsis, they require differentiation into macrophages using inducers such as PMA, which adds complexity and time to the experiments (34). Hence, the present study selected RAW 264.7 cells for *in vitro* sepsis model studies. IRAW 264.7 cells, a murine macrophage cell line derived from the ascites of male BALB/c mice with an Abelson murine leukemia virus-induced tumor, were obtained from the National Collection of Authenticated Cell Cultures (https://www.cellbank.org.cn/index.php). Cells were cultured in sterile conditions using DMEM supplemented with 10% FBS and 1% penicillin/streptomycin. Cells were then seeded into either 96- or 6-well plates and incubated at 37˚C until they reached 80-90% confluency. Following previously reported methodologies (35), an *in vitro* sepsis model was established by treating RAW 264.7 cells with 500 ng/ml of lipopolysaccharide (LPS) for 4 h to simulate bacterial infection, followed by 30 min treatment with 5 mM ATP, which mimicked the cellular damage and inflammation response observed in sepsis. DMEM, FBS, 1% penicillin/streptomycin, LPS and ATP were procured from MedChemExpress.

Cell transfection. Cell transfection was performed using Lipofectamine® 2000 (Invitrogen; Thermo Fisher Scientific, Inc.) at 37˚C for 48 h. A total of 5.0 μg of the pcDNA3.1 *MTR* overexpression (OE) vector was used, with the sequence containing both the coding region of the MTR gene (in uppercase) and necessary flanking sequences (in lowercase) as follows: forward (F) 5'-TACCGAGCTCGGATCCGCCAC CATGAAGAAAACCCTGCAGGATG-3' and reverse (R) 5'-GATATCTGCAGAATTCTCAGTCTGTGTCATAGC CCAG-3'. The negative control (NC), referred to as OE-NC, consisted of an empty pcDNA3.1 vector without any insert and was used as a baseline control to ensure the observed effects were due to MTR overexpression (Data S1). All vectors were purchased from Sangon Biotech Co., Ltd. After 48 h of transfection at 37˚C, cells were collected by centrifugation at 300 x g for 5 min at 4˚C, and the transfection efficiency was assessed using reverse transcription-quantitative PCR (RT-qPCR) and western blotting analysis.

RT-qPCR. For whole blood samples from sepsis patients and healthy controls, as well as cell lines treated with LPS and APT, including those in the control, NC-OE and OE-MTR groups, total RNA was extracted using TRIzol® reagent (Invitrogen; Thermo Fisher Scientific, Inc.) according to the manufacturer's instructions. The quality and concentration of RNA were assessed before proceeding. RNA was reverse transcribed into cDNA using the RevertAid RT Reverse Transcription Kit (Thermo Fisher Scientific, Inc.). RT-qPCR was performed using the SYBR GREEN kit (Takara Bio, Inc.). The 15 μl qPCR reaction mixture contained 1 μg RNA, 10 μl reaction solution, 1 μl RT primers (Tables II and III) and 1 μl deoxyribonucleotide triphosphates. The following thermocycling conditions were used for PCR: 95˚C for 3 min; 40 cycles of 95˚C for 30 sec, 55˚C for 30 sec and 72˚C for 30 sec. Primers were synthesized by Sangon Biotech Co., Ltd., and *GAPDH* was used as the internal reference gene. The relative expression levels of the target genes were calculated using the $2^{-\Delta\Delta Cq}$ method (36).

Table II. Primer sequences for detection of human genes.

Gene	Sequence (5'-3')
MTR	F: GAACGCCTTGAGTATGCCCTTG
	R: CCGGGCTGACTTTATAACCTGAG
MRI1	F: GCCCCGCTCCCAAGTGCGCGCGGAC
	R: GTCCGCGCGCACTTGGGAGCGGGGC
GAPDH	F: GCACCGTCAAGGCTGAGAAC
	R: TGGTGAAGACGCCAGTGGA

MTR, methionine synthase; MRI1, methionine-R-isomerase 1; F, forward; R, reverse.

Table III. Primer sequences for detection of mouse genes.

Gene	Sequence (5'-3')
MTR	F: TTCCTTTAGTCTGTCGCTGCGGCCT
	R: AGGCCGCAGCGACAGACTAAAGGAA
GAPDH	F: CTCTGAGCCTCCTCCAATTCAACCC
	R: GGGTTGAATTGGAGGAGGCTCAGAG

MTR, methionine synthase; F, forward; R, reverse.

Cell Counting Kit-8 (CCK-8) assay. RAW 264.7 cells were seeded into 96-well plates at a concentration of 8,000-10,000 cells per well, and cultured for 6, 12, 24 and 48 h at 37˚C with 5% CO_2. Following each incubation period, CCK-8 solution (Beyotime Institute of Biotechnology) was added to each well and the plates were further incubated for 2 h. Absorbance was subsequently measured at 450 nm using a microplate reader to assess cell viability.

Western blotting. Total proteins were extracted from cells using RIPA lysis buffer (Beyotime Institute of Biotechnology) and the total protein concentration was measured using a BCA assay kit (Beyotime Institute of Biotechnology). A total of 40 μg of protein was loaded per lane on a 10% gel, separated by SDS-PAGE and transferred onto PVDF membranes. Membranes were blocked with 5% fat-free milk for 1 h at room temperature and then incubated with primary antibodies against *MTR* (1:1,000; cat. no. ab66039; Abcam) and GAPDH (1:1,000; cat. no. GB12002-100; Wuhan Servicebio Technology Co., Ltd.) overnight at 4˚C. Next, membranes were treated with HRP-conjugated secondary antibodies (1:20,000; cat. no. SA00001-2; Wuhan Sanying Biotechnology Co., Ltd.) for 2 h at room temperature. Protein bands were visualized using an ECL detection kit (Wuhan Sanying Biotechnology Co., Ltd.) and protein expression levels were quantified using ImageJ software (version 1.8.0; National Institutes of Health) using GAPDH as the loading control.

Colony formation and Transwell assays. In the logarithmic growth phase, cells were detached using 0.25% trypsin, and adjusted to a concentration of $2.5x10^2$ cells/ml. Next, cells

were seeded into a 6-well plate and incubated 37˚C with 5% CO_2 for 2-3 weeks. The culture medium was changed every 3 days. After the incubation period, cells were fixed using methanol at room temperature (~25˚C) for 15 min. Following fixation, cells were stained with 1 ml of Giemsa solution at room temperature for 30 min. After staining, the cells were gently rinsed with water, and excess water was removed using filter paper. Colonies were defined as groups of at least 50 cells that were clearly distinguishable from one another. For the migration assay, a Transwell assay was conducted using 8 μm pore size Transwell inserts (Beijing Solarbio Science & Technology Co., Ltd.) without Matrigel. Briefly, $4x10^4$ cells in 200 μl FBS-free medium were added to the upper chamber, while the lower chamber was filled with 700 μl 10% FBS medium. The cells were incubated at 37˚C with 5% CO_2 for 24 h. Following incubation, cells on the lower side of the membrane were stained with Wright-Giemsa dye (Shanghai Canspec Scientific Instruments Co., Ltd.) at room temperature for 15 min. After staining, the cells were observed using a Nikon light microscope (Nikon Corp). Both colony formation and migration assays were quantified using ImageJ software (version 1.45s/Java1.6.0_20; National Institutes of Health).

Statistical analysis. All cell experiments were repeated three times to ensure reliability. The final results were presented as mean ± standard deviation. Statistical analyses and graphical presentations were performed using R (version 4.2.1) and GraphPad Prism (version 9.0; Dotmatics). Comparison analysis between groups for clinical RT-qPCR data were performed using an unpaired Student's t-test. For data involving multiple group comparisons, a one-way ANOVA followed by Tukey's post hoc test was used. The Wilcoxon rank-sum test was applied for bioinformatics data, including the comparison of MRI1 and MTR levels between the healthy group and individuals with sepsis across three datasets, as well as the comparison of different pathways between the sepsis and healthy groups. Differences in survival rates were assessed using Kaplan-Meier method and analyzed with the log-rank test. Correlations between gene expressions and pathways were analyzed using Pearson's correlation analysis. $P<0.05$ was considered to indicate a statistically significant difference.

Results

Biological analysis of the differentially expressed AAMGs. To illustrate sample differences and dataset heterogeneity, PCA was performed on each dataset (Fig. S1A-C). The clear separation indicated significant differences between patients with sepsis and healthy controls. Additionally, the datasets demonstrated distinct separations, which indicated that there was significant heterogeneity among the datasets (Fig. S1D). WGCNA was used to screen the differentially expressed genes between patients with sepsis and healthy subjects. A soft threshold of $\beta=21$ was selected to construct a scale-free network (Fig. 2A). Through this analysis, 11 gene modules were acquired (Fig. 2B), with the magenta module showing the highest association with sepsis ($r=-5.77$; $P<0.05$; Fig. 2C). The genes within this module exhibited a significant correlation with the gene expression profiles of patients with sepsis ($r=0.49$; $P<0.05$; Fig. 2D). In total, 211 AAMGs that were differentially expressed between sepsis and healthy subjects were identified and visualized using a heatmap (Fig. 3A) and volcano plot (Fig. 3B). From these, 34 AAMGs were obtained at the intersections of genes in the magenta module and differentially expressed AAMGs (Fig. 3C). GO analysis demonstrated enrichment of these genes in AAM (Fig. 3D). Additionally, KEGG analysis presented pathways, including aminoacyl-transfer RNA (tRNA) biosynthesis and cysteine and methionine metabolism, associated with these genes (Fig. 3E). DO analysis further confirmed that these 34 AAMGs were enriched in amino acid metabolic disorder (Fig. 3F). These results collectively demonstrated the close association between 34 AAMGs and AAM in sepsis.

Identification of hub AAMGs. Machine learning algorithms are increasingly prevalent for identifying robust diagnosis biomarkers in bioinformatics analysis (37). In the present study, these methods were performed to screen for hub AAMGs in sepsis. Using LASSO, SVM-RFE and RF algorithms, 22, 21 and 13 candidate AAMGs were identified, respectively (Fig. 4A-C). Through a Venn diagram analysis, an overlap among results of these machine learning algorithms showed four potential AAMGs as diagnostic candidates, namely *MRI1*, *MTR*, *MYC* and quinoid dihydropteridine reductase (*QDPR*) (Fig. 4D). To verify the robustness of theses AAMGs in sepsis, their expressions levels across three cohorts of healthy subjects and patients with sepsis were assessed. While the expression levels of *MRI1* and *MTR* remained consistent across all three cohorts, *MYC* and *QDPR* showed decreased expression in sepsis compared with healthy controls in the GSE65682 and GSE185263 cohorts. However, *MYC* was undetected and *QDPR* expression levels demonstrated no significant differences between healthy subjects and patients with sepsis in the GSE154918 cohort (Fig. 5). Although elevated methylation levels in *MRI1* have been observed in patients with severe asthma (38) and genetic polymorphisms in *MTR* have been strongly linked to various diseases (39,40), their roles in sepsis remain understudied. Thus, *MRI1* and *MTR* were selected as the hub AAMGs for further analysis.

Diagnostic and prognostic value of hub AAMGs in sepsis. Similar to a previous study (41) on the diagnostic value of certain biomarkers for sepsis, the present study also demonstrated the potential diagnostic value of hub AAMGS (*MRI1* and *MTR*) for sepsis. A nomogram was constructed based on the expression levels of *MRI1* and *MTR* (Fig. 6A-C) and the AUC values of each gene and the nomogram were evaluated across the three cohorts. *MRI1, MTR* and the nomogram all exhibited consistently high diagnostic values for sepsis in the GSE65682 (AUC=0.969, 0.982 and 0.989, respectively), GSE154918 (AUC=0.886, 0.981 and 0.981, respectively) and GSE185263 datasets (AUC=0.884, 0.944 and 0.958, respectively) (Fig. 6D-F). Given the diagnostic value of the two AAMGs, their prognostic predictive value in sepsis was further explored. Patients with sepsis were divided into a high-expression group and a low-expression group according to the best cutoff point. The high-expression *MTR* group had a better prognosis than the low-expression *MTR* group (Fig. 7A), and this result was confirmed in the internal validation assay (Fig. 7D). Similar results were observed for *MRI1* (Fig. 7B and E). Furthermore,

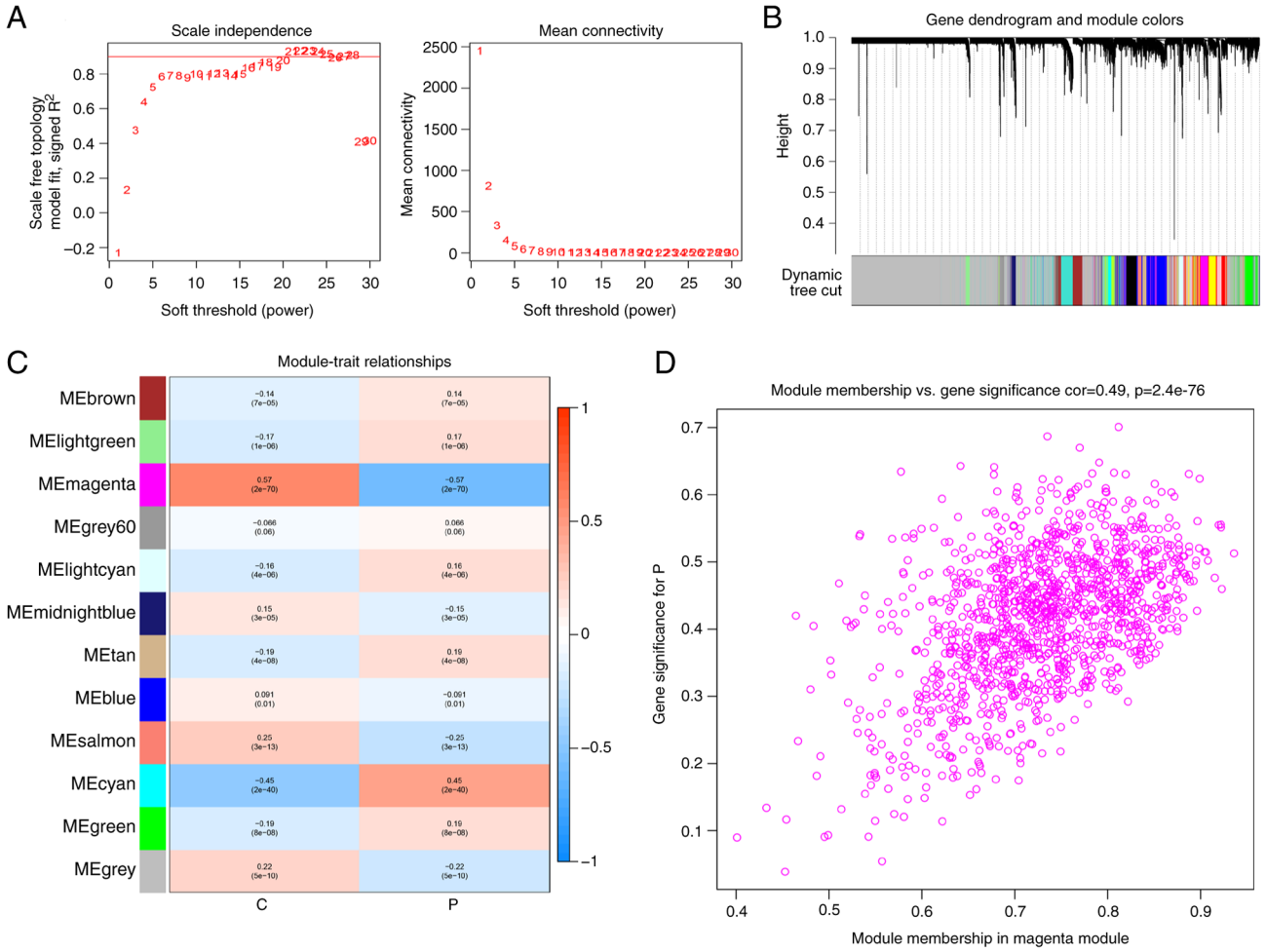

Figure 2. WGCNA identifies the module with the strongest correlation to sepsis. (A) Network topology analysis under various soft-threshold powers. (B) Clustering dendrogram of genes with different similarities based on topological overlap and assigned module color. (C) Module-trait association. Each row corresponded to a module while each column corresponded to a feature. Correlations and corresponding P-values (in parentheses) are provided for each module. (D) Relevance of members in the magenta module with sepsis. ME, module membership; C, control; P, patient with sepsis.

among the four groups, those with high expression levels of both *MTR* and *MRI1* exhibited the most favorable prognosis, whereas the opposite was observed for those with low expression levels of both *MTR* and *MRI1* (Fig. 7C and F). To further validate the diagnostic and prognostic models constructed in the present study, external patient cohorts were used, specifically GSE95233 (22 healthy samples and 102 sepsis samples) and GSE4607 (15 healthy samples and 108 sepsis samples). The diagnostic model results demonstrated that *MRI1*, *MTR* and the nomogram maintained high diagnostic value for sepsis. In GSE95233, the AUC values for *MRI1*, *MTR* and the nomogram were 0.963, 0.972 and 0.987, respectively, and in GSE4607, the AUC values were 0.845, 0.864 and 0.879, respectively (data not shown). However, the prognostic model did not perform well, demonstrating no significant difference in survival time between the high and low expression groups for *MTR* and *MRI1* in both datasets (data not shown). Overall, *MRI1* and *MTR* demonstrated robust diagnostic and prognosis values for patients with sepsis, and they could potentially be used as predictive prognostic factors for patients with sepsis.

Biological functions, potential pathways and immune cell infiltration analysis of MRI1 and MTR in sepsis. Given the demonstrated diagnostic and prognosis values of *MRI1* and *MTR* in sepsis, ssGSEA was utilized to clarify their potential roles. Activation of immune-related diseases, including allograft rejection, asthma and autoimmune thyroid disease, were observed with both *MRI1* and *MTR* (Fig. 8A and D). Conversely, metabolic pathways such as fatty acid biosynthesis and glycosphingolipid biosynthesis were inhibited with *MRI1* and *MTR* expression. Additionally, significant associations were found between *MRI1* and *MTR* expression and various inflammation-related pathways, such as *PI3K/AKT/mTOR* signaling, *IL-6/JAK/STAT3* signaling and hypoxia, which highlights their potential role in sepsis (Fig. 8B). Given the high mortality rate of sepsis, identifying effective treatment methods is imperative. Thus, potential pathways associated with sepsis were explored to identify novel targets. Apart from oxidative phosphorylation, complement and hedgehog signaling, all other pathways showed significant differences between healthy subjects and patients with sepsis (Fig. 8C). Some known pathways, such as *PI3K/AKT/mTOR* (42), *p53* (43), *Notch* (44) and hypoxia (45), have been previously reported to have a strong association with sepsis. Additionally, novel pathways such as *KRAS* and *IL2/STAT5* were first reported in the current study. This expansion of our understanding

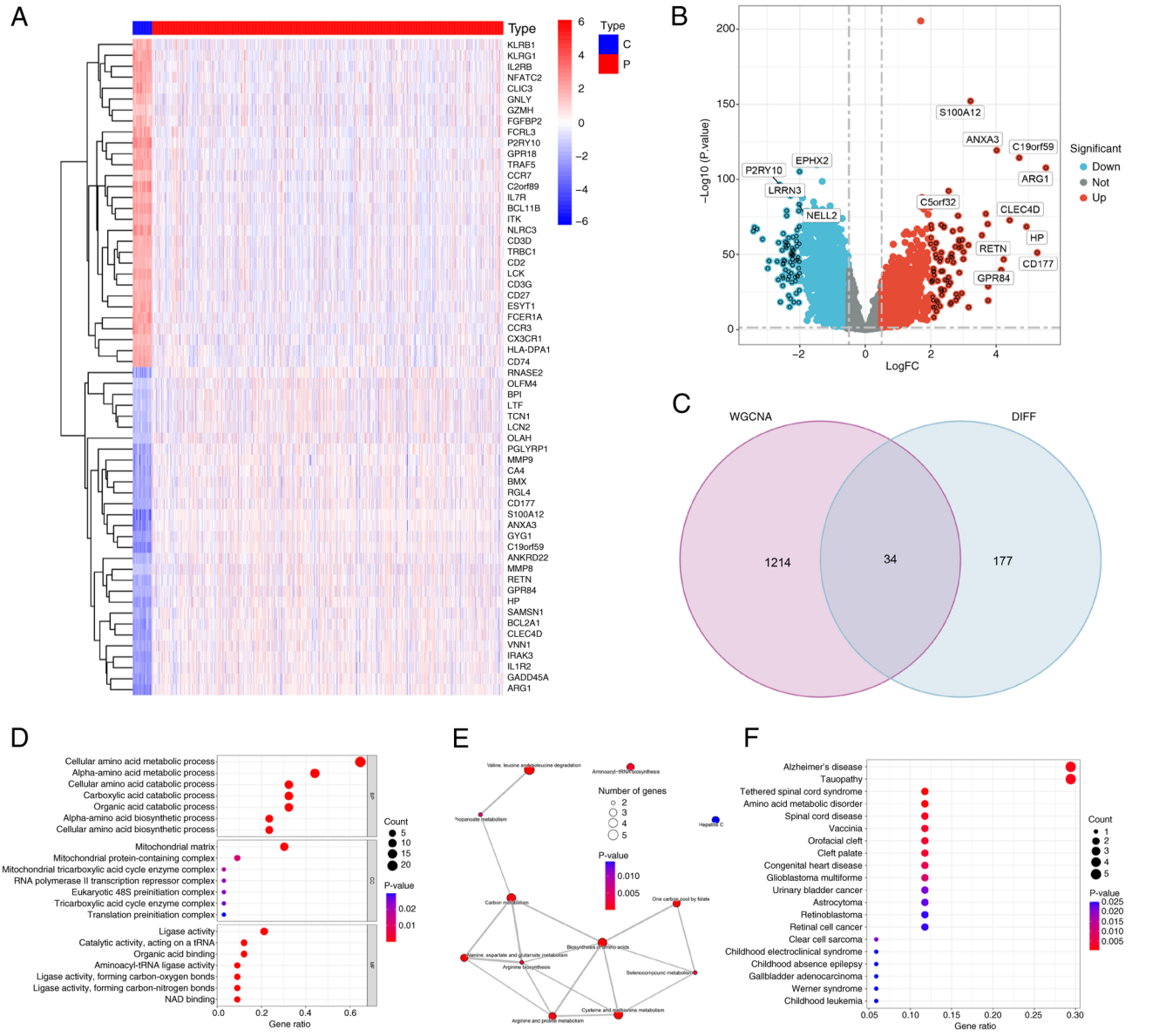

Figure 3. Biological functions of differentially expressed AAMGs. (A) Heatmap and (B) volcano plots of differently expressed AAMGs between sepsis and healthy groups. (C) Venn diagram showing the intersection of WGCNA and DIFF AAMGs. (D) Gene Ontology, (E) Kyoto Encyclopedia of Genes and Genome and (F) Disease Ontology analysis of the 34 AAMGs. C, control; P, patient with sepsis; AAMGS, amino acid metabolism-related genes; WGCNA, weighted gene co-expression network analysis; DIFF, differentially expressed.

of sepsis-related pathways underscores the complexity of its pathophysiology and highlights the need to explore further how these pathways influence immune responses. To this end, considering the crucial role of immune cells in sepsis, the CIBERSORT algorithm was further applied to analyze the associations between *MRI1*, *MTR* and immune cell infiltration. The present findings demonstrated that these genes were negatively correlated with the infiltration of pro-inflammatory cells, such as M1 macrophages, neutrophils and eosinophils, while exhibiting positive correlations with anti-inflammatory cells, such as activated natural killer, $CD8^+$ T and dendritic cells (Fig. 9A and B). Collectively, the current study identified *MRI1* and *MTR* as potential promising therapeutic targets for sepsis treatment, providing a foundation for further exploration into their roles in modulating immune responses in this complex condition.

Role of AAMGs in sepsis. Further validation was conducted using samples from five patients with sepsis and five healthy individuals from Xianning Central Hospital (Hubei, China) to verify the expression trends of *MRI1* and *MTR*. The results indicated that both genes were downregulated in the peripheral blood of patients with sepsis compared with healthy individuals (Fig. 10A). As *MTR* exhibited consistently high diagnostic values for sepsis in the aforementioned three datasets (all AUC>0.94), the present study focused on the mechanism of *MTR* in sepsis. In an *in vitro* sepsis model induced by LPS and ATP, the mRNA expression levels of *MTR* and cell viability gradually decreased over time at 6, 12, 24 and 48 h compared with the control group (all P<0.05) (Fig. 10B and D). Subsequently, RAW 264.7 cells were transfected with MTR-OE plasmid. The RT-qPCR and western blot results demonstrated that the MTR mRNA and protein

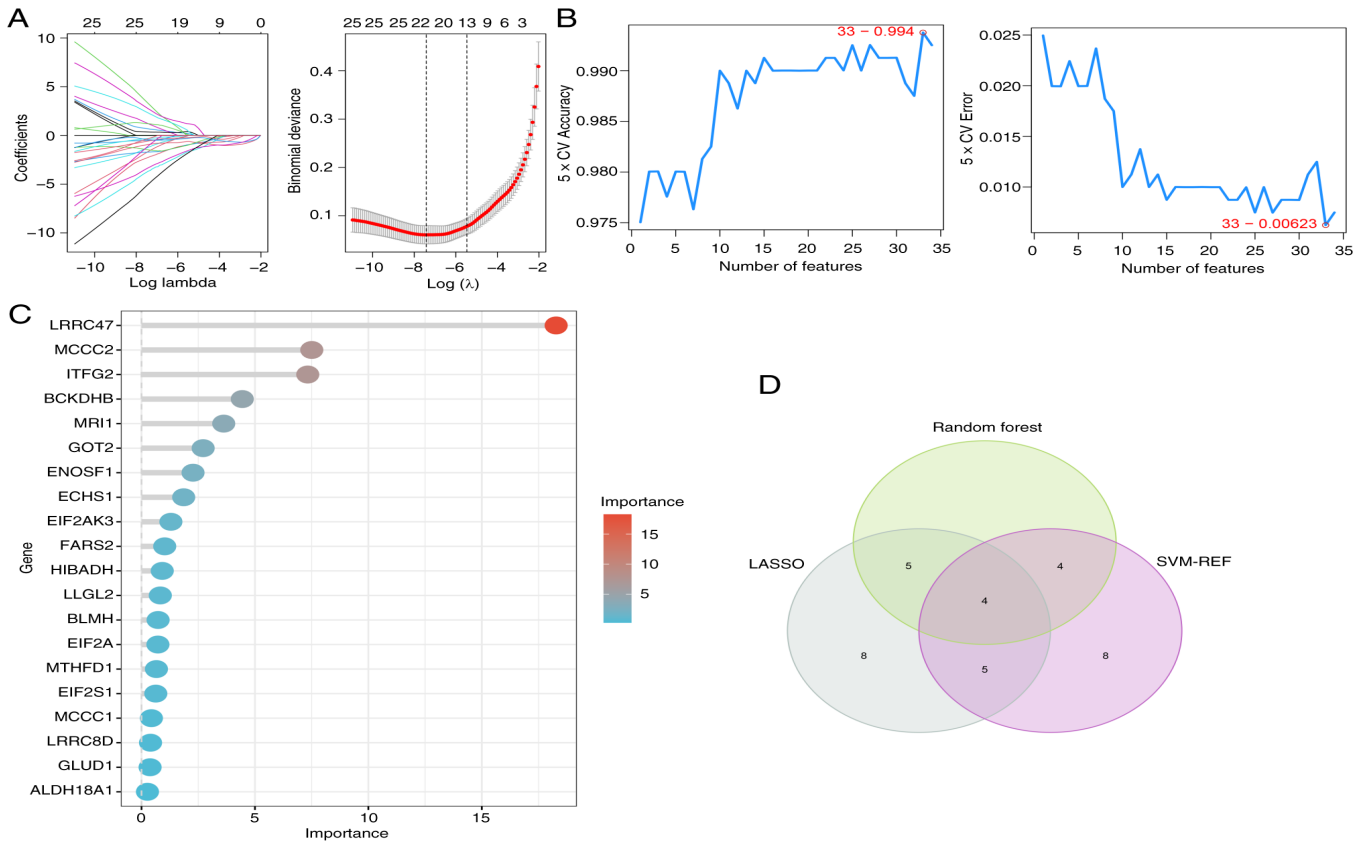

Figure 4. Identification of hub AAMGs through machine learning. AAMGs screening in a three machine learning algorithms model, which included (A) LASSO, (B) SVM-REF and (C) random forest. (D) Venn diagram showing that four candidates diagnostic AAMGs were identified via the aforementioned three algorithms. AAMGS, amino acid metabolism-related genes; LASSO, least absolute shrinkage and selection operator; SVM-RFE, support vector machine-recursive feature elimination.

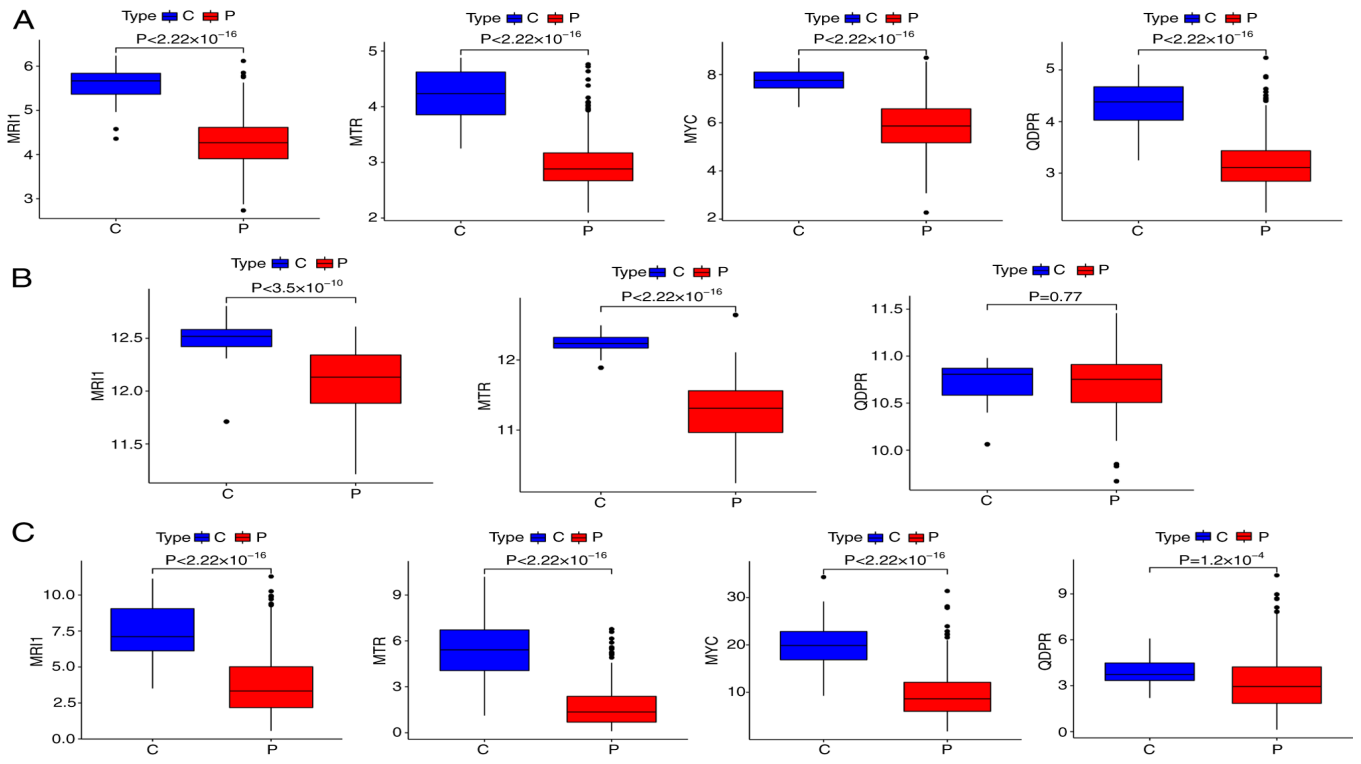

Figure 5. Expression patterns of hub AAMGs across different datasets. Boxplots showing the differences in expression levels of MRI1, MTR, MYC and QDPR between the sepsis and healthy groups in the (A) GSE65682, (B) GSE154918 and (C) GSE185263 datasets. Data are presented as mean with standard deviation. MRI1, methylthioribose-1-phosphate isomerase 1; MTR, methionine synthase; MYC, MYC proto-oncogene; QDPR, quinoid dihydropteridine reductase; C, control; P, patient with sepsis.

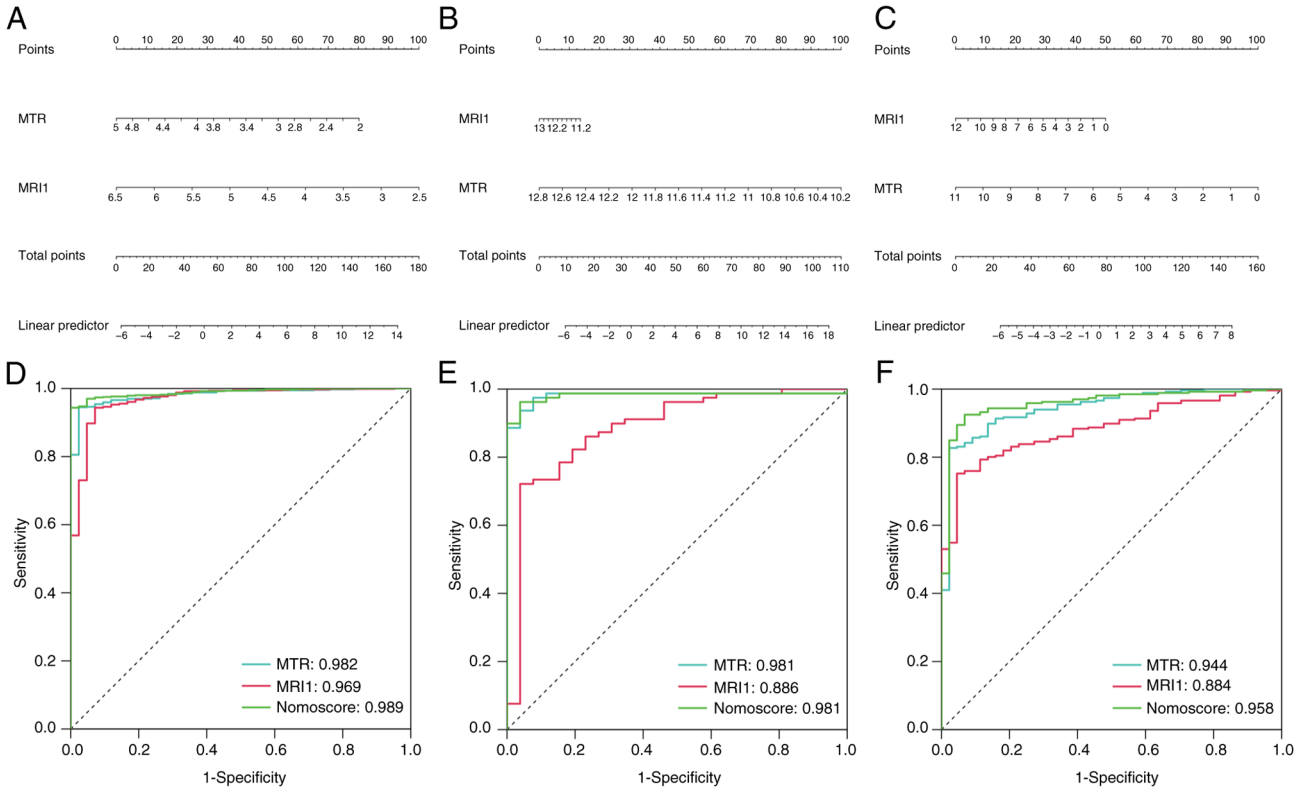

Figure 6. Diagnostic value of MTR and MRI1 in sepsis. Nomograms of the (A) GSE65682, (B) GSE154918 and (C) GSE185263 datasets for diagnosing sepsis. Receiver operating characteristic curve of MTR and MRI1 and nomograms showed the diagnostic values of MTR and MRI1 in (D) GSE65682, (E) GSE154918 and (F) GSE185263 datasets. MTR, methionine synthase; MRI1, methylthioribose-1-phosphate isomerase 1.

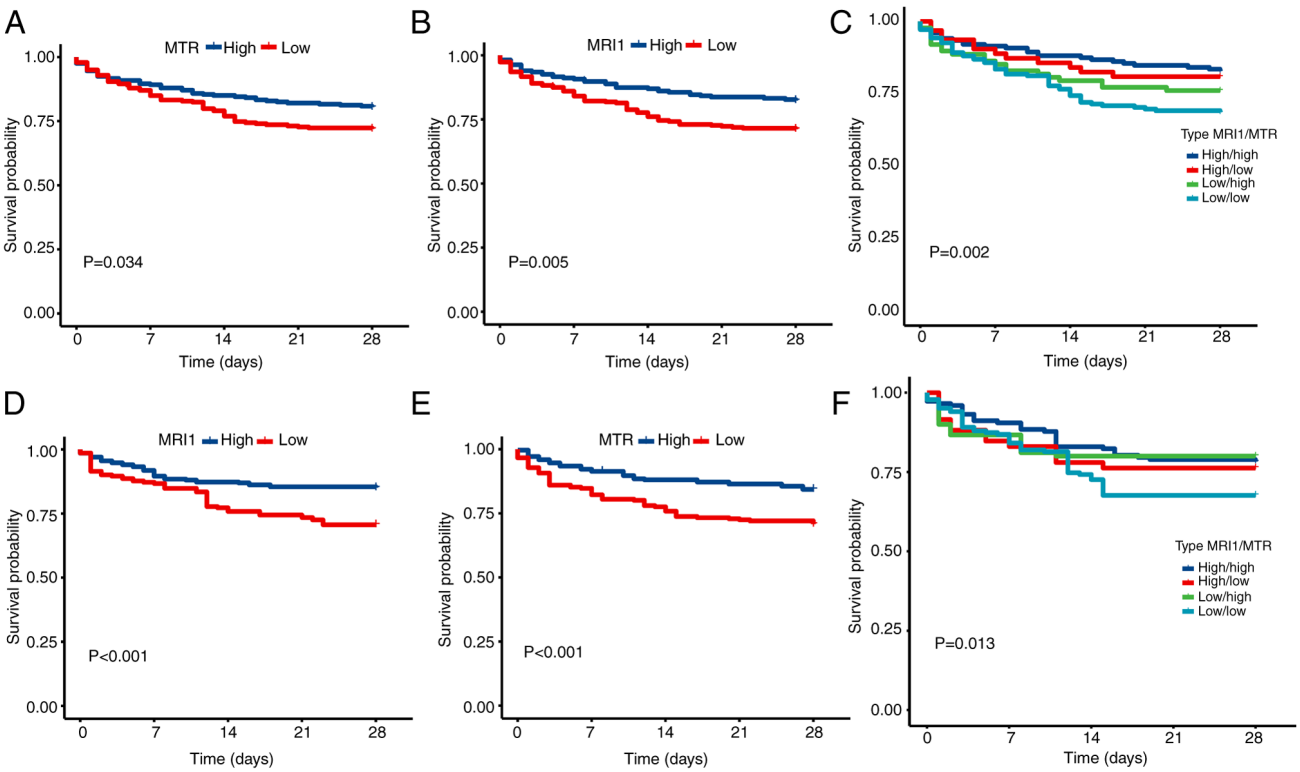

Figure 7. Prognostic predictive value of MTR and MRI1 in sepsis. (A) Kaplan-Meier survival curve based on the expression of MTR in the GSE65682 cohort. (B) Kaplan-Meier survival curve based on the expression of MRI1 in the GSE65682 cohort. (C) Kaplan-Meier survival curve based on the combined expression of MTR and MRI1 in the GSE65682 cohort. (D) Kaplan-Meier survival curve for MTR expression, specifically in the internal validation subset of the GSE65682 cohort. (E) Kaplan-Meier survival curve for MRI1 expression in the internal validation subset of the GSE65682 cohort. (F) Kaplan-Meier survival curve for the combined expression of MTR and MRI1 in the internal validation subset of the GSE65682 cohort. MTR, Methionine synthase; MRI1, methylthioribose-1-phosphate isomerase 1.

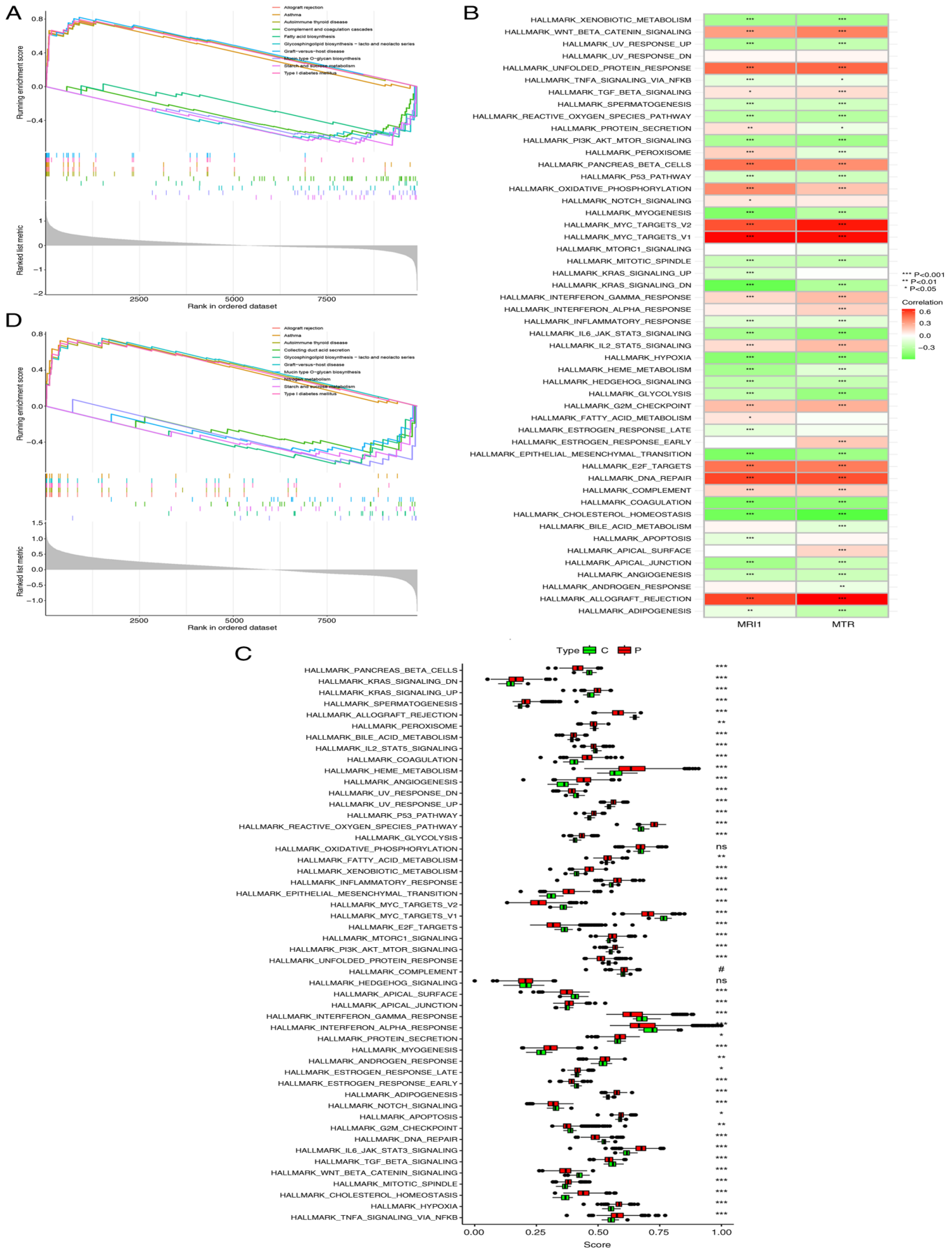

Figure 8. Potential biological functions of MTR and MRI1. (A) Gene set enrichment analysis plot of the top five pathways in MTR. (B) Pathways associated with MTR and MRI1. (C) Boxplots presenting the differences between sepsis and healthy groups. (D) Gene set enrichment analysis plot of the top five pathways in MRI1. Data are presented as mean with standard deviation. *P<0.05, **P<0.01, ***P<0.001. ns, not significant. MTR, Methionine synthase; MRI1, methylthioribose-1-phosphate isomerase 1; C, control; P, patient with sepsis.

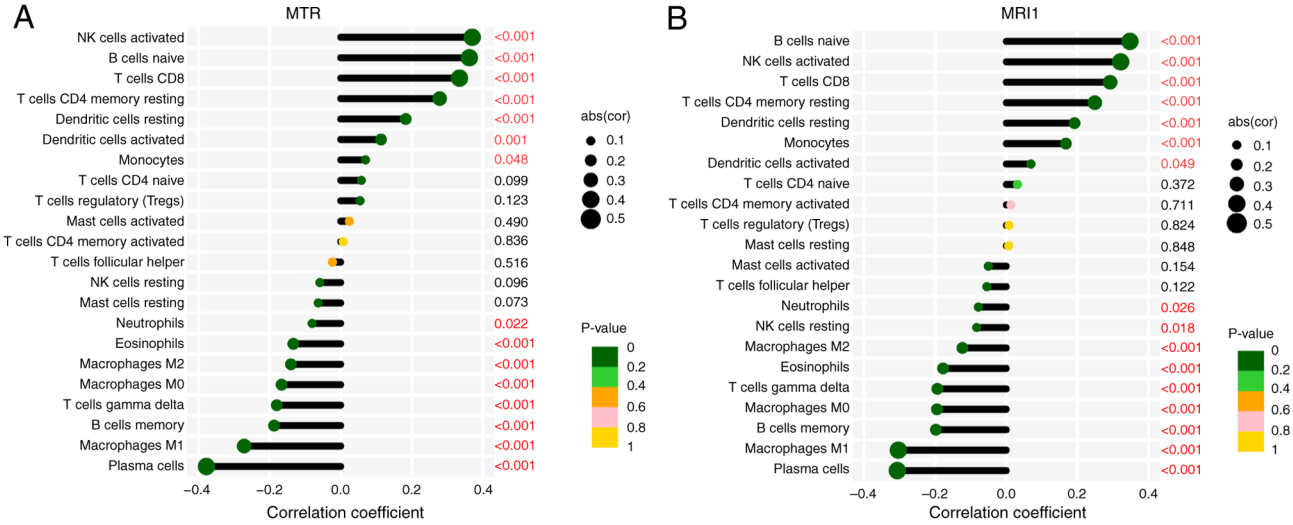

Figure 9. Relationship between MTR and MRI1 expression levels and immune cell infiltration abundance in Sepsis. Lollipop charts of the correlation between immune cell infiltration abundance and the expression levels of (A) MTR and (B) MRI1. Data are presented as mean with standard deviation. MTR, Methionine synthase; MRI1, methylthioribose-1-phosphate isomerase 1; abs(cor), the absolute value of the correlation coefficient.

expression levels in the transfected cell line were higher than those compared with the control and NC-OE groups (Fig. 10C), which confirmed successful construction of the MTR-OE plasmid. Further experiments using LPS and ATP to simulate sepsis *in vitro* showed that, compared with the control group, MTR protein expression decreased after 4 h of LPS stimulation followed by 30 min of ATP treatment (Fig. 10E). By contrast, the cell line transfected with the MTR-OE plasmid exhibited increased MTR protein levels compared with the NC-OE group. Additionally, LPS and ATP gradually inhibited cell clonogenic and proliferative abilities, whereas MTR-OE treatment reversed these trends (all $P<0.05$) (Fig. 10F and G). In summary, these findings suggested that MTR may serve a protective role in the LPS and ATP-induced sepsis model.

Discussion

Sepsis is a critical medical condition characterized by high incidence and mortality rates (2). The need for biomarkers with strong diagnostic and prognostic predictive value has emerged as a central focus in contemporary sepsis research. Previously, widely-used machine learning algorithms, such as WGCNA, LASSO, SVM-RFE and RF analysis, have facilitated the identification of key genes for sepsis biomarkers (46,47). For instance, Dai *et al* (48) employed WGCNA to identify *LPIN1* as a potential biomarker for sepsis, while another study combined LASSO, SVM-RFE and RF algorithms to screen for four sensitive diagnostic genes for sepsis (17). In the present study, WGCNA, LASSO, SVM-RFE and RF analyses were integrated. WGCNA focuses on specific phenotypes and co-expression modules, where genes within the same module are functionally related and biologically significant (49). LASSO enhances model performance by effectively selecting features and addressing multicollinearity issues (50). SVM-RFE optimizes feature selection by recursively eliminating unimportant features (51), while RF evaluates the importance of variables in classification (52). Traditional bioinformatics analyses rely on manually designed rules and processes, which can introduce subjectivity and limitations, potentially hindering the discovery of patterns and information within the data and making it difficult to handle complex data structures and relationships (53). The present study combined WGCNA, LASSO, SVM-RFE and RF algorithms to enable the identification of more efficient biomarkers for sepsis, which resulted in the identification of two AAMGs, *MTR* and *MIR1*. These genes exhibited downregulated expression in patients with sepsis across various public datasets and clinical samples and were demonstrated to be valuable for both diagnostic and prognostic purposes. Additionally, the current study demonstrated that *MTR* and *MIR1* were closely associated with certain pathways, such as *KRAS* and *IL2/STAT5*, as well as immune cell infiltration, including M1 macrophages and neutrophils. Collectively, the present findings potentially offer a novel approach to sepsis biomarker identification with high sensitivity and reliability, thus providing a promising avenue for sepsis diagnosis and prognosis.

A number of previous *in vitro* and *in vivo* studies have elucidated the mechanisms underlying AAM in sepsis. These studies have reported significant reductions in muscle amino acid uptake, which is regulated by various circulating factors such as growth hormone, cytokines like *TNF-α* and *IL-6*, stress hormones including cortisol, and metabolic regulators such as insulin (54), as well as impaired leucine-induced *mTOR* activation in muscles during sepsis (55). To the best of our knowledge, bioinformatics analysis was applied for the first time to evaluate the diagnostic and prognostic value of AAMGs in patients with sepsis. The present study identified two AAMGs, *MTR* and *MIR1*, with high diagnostic value across all three publicly available datasets. Moreover, additional analyses were conducted to determine their prognostic significance. Although *MTR* and *MIR1* did not show prognostic predictive value for sepsis in the GSE95233 and GSE4607 datasets, this lack of performance could potentially be attributed to the short follow-up duration in these datasets, which was only 3 days. Furthermore, considering that previous studies lacked internal validation or randomized splitting (56),

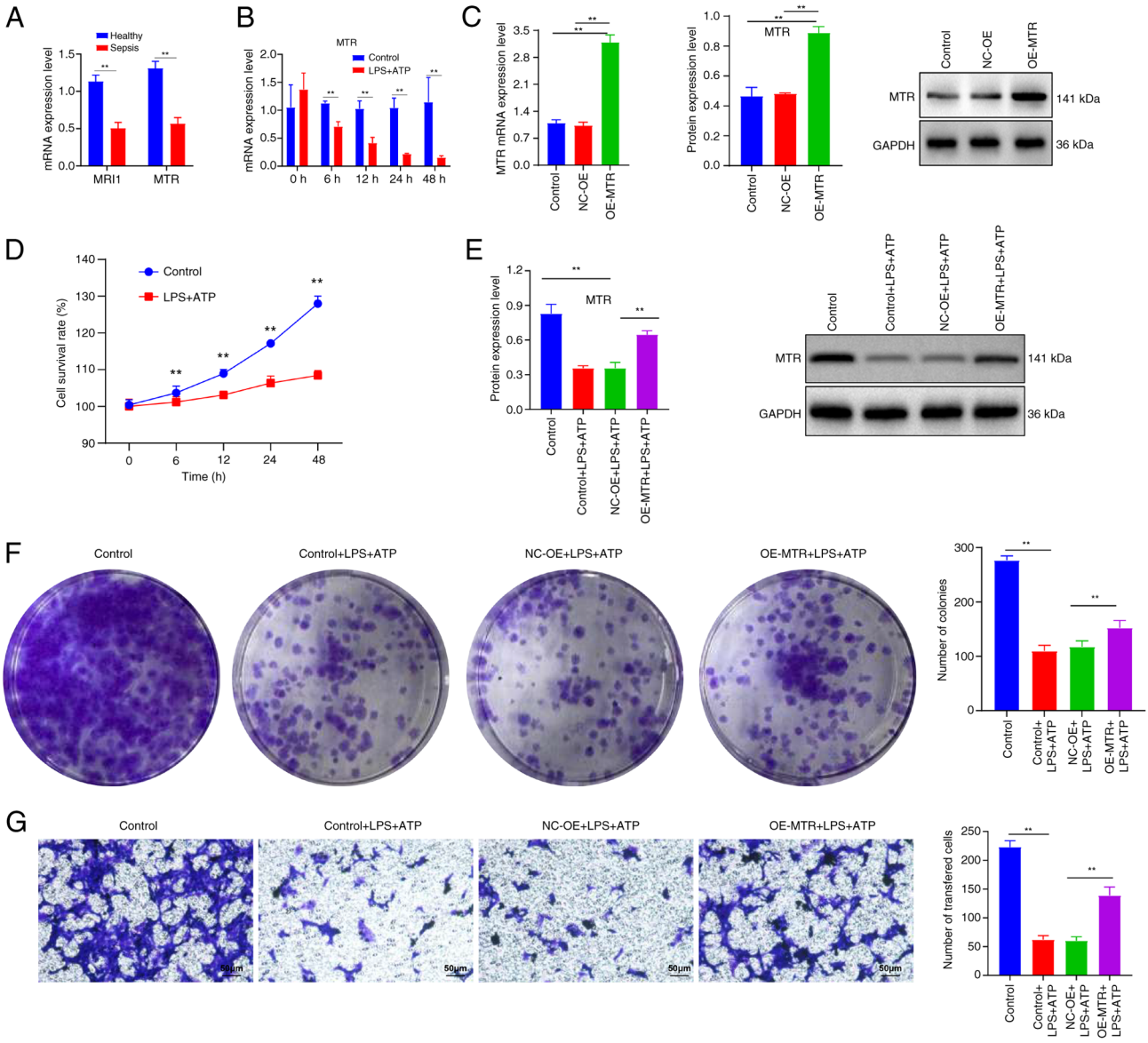

Figure 10. The role of MTR in sepsis. (A) Comparison of mRNA expression levels of MTR and MRI1 in peripheral blood samples between five patients with sepsis and five healthy individuals. (B) mRNA expression level of MTR between the control and LPS + ATP-induced groups. (C) mRNA and protein expression levels of MTR in cells transfected with different vectors. (D) Differences in cell survival rate between the control and LPS + ATP-induced groups (**P<0.01 vs. LPS + ATP group). (E) Protein expression levels of MTR across cells transfected with different vectors. Comparison of (F) colony formation and (G) proliferation rates among cells transfected with different vectors (scale bar, 50 μm). **P<0.01. LPS, lipopolysaccharide; MTR, methionine synthase; OE, overexpression; NC, negative control.

the present study employed a more reliable bootstrap approach, which confirmed the robust prognostic predictive ability of *MTR* and *MIR1* in patients with sepsis. Clinical samples from a local hospital also supported the trend of reduced expression of *MTR* and *MIR1* in the peripheral blood of patients with sepsis compared with healthy individuals, which may potentially provide a solid foundation for the development of personalized treatment plans in future clinical practice. Furthermore, *in vitro* experiments involving the overexpression of *MTR* demonstrated its potential to mitigate LPS-induced damage, which further supported the consistency and validity of the aforementioned findings.

Currently, research on *MTR* and *MIR1* in the context of sepsis is limited. Considering that *MTR* is a critical enzyme responsible for converting homocysteine to methionine in methylation reactions and *MIR1* acts as methionyl-tRNA synthetase 1, their potential mechanisms of action in sepsis may involve the regulation of methionine metabolism (57). A previous study reported that levels of methionine and its derivatives, particularly N-formyl-L-methionine, were significantly elevated in the plasma of patients with septic shock compared to those with cardiogenic shock or non-septic bacteremia and healthy controls (6). Furthermore, the methionine cycle and its associated antioxidant and anti-inflammatory processes may present new potential targets for the treatment of sepsis (58). Methionine sulfoxide, an oxidized form of methionine, has been recognized as a biomarker in the progression of sepsis and subsequent acute kidney injury (59). Furthermore, methionine and certain immune cells serve a role in impacting the development of

sepsis. For instance, in *in vivo* models of sepsis, the oxidation of methionine exacerbates the release of pro-inflammatory mediators and the inflammatory response by altering macrophage metabolism towards glycolysis and increasing reactive oxygen species levels (60). The methionine pathway is also inhibited by the long non-coding RNA *MALAT1*, which in turn increases the levels of pro-inflammatory cytokines and the antioxidant capacity of macrophages, thereby exacerbating the inflammatory response in sepsis (58). These findings underscore the research potential of methionine in sepsis and provide direction for further investigation into the specific roles of *MTR* and *MIR1* in AAM within the context of sepsis.

Furthermore, the present study demonstrated that *MTR* and *MIR1* were negatively correlated with signaling pathways such as *PI3K/AKT/mTOR*, whose activation has been reported by a number of previous studies to mitigate the severity of sepsis (61,62). The *PI3K/AKT/mTOR* pathway regulates cellular metabolism, proliferation and survival, and its activation leads to the suppression of pro-inflammatory cytokine production and the enhancement of anti-inflammatory cytokines, thereby reducing the severity of sepsis (63,64). In the present study, two pathways previously unreported in sepsis research were also identified, namely the *KRAS* and *IL2/STAT5* pathways. *KRAS* activation leads to the phosphorylation of *MAPK*, which in turn activates transcription factors such as *NF-κB* (65). *NF-κB* then translocates to the nucleus and promotes the transcription of pro-inflammatory cytokines, including *TNF-α* and *IL-6*, which serve crucial roles in the inflammatory response in sepsis by promoting systemic inflammation, fever and tissue damage (66-70). Furthermore, the *IL2/STAT5* pathway serves a critical role in regulating the immune response, particularly the T cell response in sepsis. Binding of *IL-2* to its receptor leads to the activation of *JAK3*, which phosphorylates *STAT5*. Activated *STAT5* dimerizes and translocates to the nucleus, where it promotes the expression of genes involved in T cell proliferation, differentiation and survival (71). This enhances the immune system's response to infection by increasing the number and activity of T cells, which are essential for clearing pathogens and modulating the immune response in sepsis (72). Additionally, the interaction between immune cells and AAM serves a crucial role in sepsis. For instance, it has been reported that, when macrophages are stimulated by α-aminobutyric acid, oxidative phosphorylation and the metabolism of glutamine and arginine are activated, thereby inhibiting the polarization of M1 macrophages and ultimately prolonging the survival time of mice with sepsis (73). Another previous study reported that L-lysine could regulate the neutrophil and lymphocyte counts in the peripheral blood of animal models with sepsis-induced acute lung injury (74). Glutamine has been shown to balance the polarization of T helper cells in the blood of patients with sepsis, maintain T cell populations, prevent splenic $CD4^+$ T cell apoptosis and reduce late-stage kidney injury in polymicrobial sepsis (75).

Given the importance of immune cells and AAM in sepsis, the association between *MTR* and *MIR1* and immune cells was further analyzed in the present study. These results demonstrated that *MTR* and *MIR1* were negatively correlated with the infiltration of pro-inflammatory cells, such as neutrophils and M1 macrophages, and were positively correlated with anti-inflammatory cells, such as $CD8^+$ T and dendritic cells. Specific immune cells, neutrophils, M1 macrophages, $CD8^+$ T cells and dendritic cells, are closely associated with sepsis, laying the foundation for research targeting *MTR* and *MIR1* to modulate immune cell responses in sepsis (76-80). Overall, these findings support the research potential of *MTR* and *MIR1* in sepsis and provide direction for further investigation into their specific mechanisms of action.

Although the present study has filled a gap in research regarding AAMGs in sepsis, it is not without limitations. Firstly, despite using multiple datasets for validation and applying standardized preprocessing procedures to minimize batch effects and heterogeneity, inherent variations between datasets, including differences in sample collection, processing methods and demographic disparities, could still impact the results. The preprocessing steps included averaging the expression values of the same gene and removing values ≤0. PCA was conducted on each dataset individually to compare the distribution differences between the sepsis and healthy groups, which ensured significant distribution differences before further analysis. Since datasets for analysis were not merged, batch effect correction methods such as Combat were not applied. The PCA results indicated significant heterogeneity between datasets, potentially confounding the present findings. Specifically, different sample collection methods may lead to variations in gene expression levels, with potential contamination or degradation affecting measurements. Processing protocol differences among laboratories, such as storage conditions, extraction methods and sequencing technologies, could reduce data consistency. Different sequencing platforms may have varying sequencing depths and accuracies, which may impact data comparability. Patient demographics such as age, sex and disease severity could differ between datasets, influencing gene expression and confounding the identification of sepsis-related genes. Future studies should integrate data from multiple centers, standardize sample processing and sequencing methods, and account for clinical factors such as age and infection-related variables to reduce batch effects and heterogeneity, enhancing research credibility. Furthermore, while machine learning algorithms exhibit excellent performance in feature selection and classification, they also have certain limitations. The interpretability of machine learning models is often lower compared with traditional statistical models, which typically have simpler, more transparent mechanisms that are easier to directly understand and explain (81). In the present study, various machine learning algorithms such as LASSO, SVM-RFE and RF were used, which, although improving the efficiency of feature selection, also increased model complexity. Therefore, future research needs larger datasets and more extensive validation to ensure the generalizability and robustness of the models. The current validation using local data was limited by a small sample size and single-center origin, which may affect the robustness of the present findings; thus, expanding sample sizes and including multicenter studies are essential. Additionally, while the present *in vitro* experiments provided preliminary evidence, they did not explore downstream mechanisms in depth. It was identified that *MTR* and *MIR1* may regulate methionine metabolism

in sepsis and may be associated with certain immune cells, but these mechanisms were not validated through further experiments. Future research should investigate the specific mechanisms of action of these genes to better understand their roles and applications in sepsis.

In conclusion, the present study identified *MTR* and *MIR1* as potential promising diagnostic and prognostic biomarkers for sepsis. These genes were linked with critical signaling pathways, including *KRAS* and *IL2/STAT5,* and correlated with the infiltration of immune cells, such as M1 macrophages and neutrophils. By modulating methionine metabolism, *MTR* and *MIR1* may serve a pivotal role in sepsis pathophysiology.

Acknowledgements

Not applicable.

Funding

The present study was supported by the Scientific Research Fund of The First Affiliated Hospital of Hubei University of Science and Technology (Xianning Central Hospital; grant no. 2021XYBO11).

Availability of data and materials

The data supporting the findings of the present study are openly available in the GEO repository (www.ncbi.nlm.nih.gov/gds/). This includes three microarray datasets, specifically GSE65682 (https://www.ncbi.nlm.nih.gov/geo/query/acc.cgi?), GSE154918 (https://www.ncbi.nlm.nih.gov/geo/query/acc.cgi?) and GSE185263 (https://www.ncbi.nlm.nih.gov/geo/query/acc.cgi?). The data generated in the present study may be requested from the corresponding author.

Authors' contributions

YW and QL designed the study, QL wrote the manuscript and acquired the data, YW and WX produced the figures, YW and WX performed the experiments and analyzed the data, YW and QL confirm the authenticity of all the raw data. All authors read and approved the final version of the manuscript.

Ethics approval and consent to participate

Adhering to the ethical guidelines of the Declaration of Helsinki, the present study was approved by the Ethics Committee of Xianning Central Hospital (Xianning, China) [approval no. K (2024)005]. Written informed consent was obtained from all the participants.

Patient consent for publication

Not applicable.

Competing interests

The authors declare that they have no competing interests.

Reference

1. Becker JU, Theodosis C, Jacob ST, Wira CR and Groce NE: Surviving sepsis in low-income and middle-income countries: New directions for care and research. Lancet Infect Dis 9: 577-582, 2009.
2. Fleischmann C, Scherag A, Adhikari NKJ, Hartog CS, Tsaganos T, Schlattmann P, Angus DC and Reinhart K; International Forum of Acute Care Trialists: Assessment of global incidence and mortality of hospital-treated sepsis. Current estimates and limitations. Am J Respir Crit Care Med 193: 259-272, 2016.
3. Guliciuc M, Porav-Hodade D, Chibelean BC, Voidazan ST, Ghirca VM, Maier AC, Marinescu M and Firescu D: The role of biomarkers and scores in describing urosepsis. Medicina (Kaunas) 59: 597, 2023.
4. Dai W, Shen J, Yan J, Bott AJ, Maimouni S, Daguplo HQ, Wang Y, Khayati K, Guo JY, Zhang L, *et al*: Glutamine synthetase limits β-catenin-mutated liver cancer growth by maintaining nitrogen homeostasis and suppressing mTORC1. J Clin Invest 132: e161408, 2022.
5. Sivanand S and Vander Heiden MG: Emerging roles for branched-chain amino acid metabolism in cancer. Cancer Cell 37: 147-156, 2020.
6. Rogers RS, Sharma R, Shah HB, Skinner OS, Guo XA, Panda A, Gupta R, Durham TJ, Shaughnessy KB, Mayers JR, *et al*: Circulating N-lactoyl-amino acids and N-formyl-methionine reflect mitochondrial dysfunction and predict mortality in septic shock. Metabolomics 20: 36, 2024.
7. Yang Y, Chen Q, Fan S, Lu Y, Huang Q, Liu X and Peng X: Glutamine sustains energy metabolism and alleviates liver injury in burn sepsis by promoting the assembly of mitochondrial HSP60-HSP10 complex via SIRT4 dependent protein deacetylation. Redox Rep 29: 2312320, 2024.
8. Peng X, Zheng T, Guo Y and Zhu Y: Amino acid metabolism genes associated with immunotherapy responses and clinical prognosis of colorectal cancer. Front Mol Biosci 9: 955705, 2022.
9. Shi H, Yuan X, Yang X, Huang R, Fan W and Liu G: A novel diabetic foot ulcer diagnostic model: Identification and analysis of genes related to glutamine metabolism and immune infiltration. BMC Genomics 25: 125, 2024.
10. Choi H, Lee JY, Yoo H and Jeon K: Bioinformatics analysis of gene expression profiles for diagnosing sepsis and risk prediction in patients with sepsis. Int J Mol Sci 24: 9362, 2023.
11. Xu X, Bu B, Tian H, Wu R and Yang J: MicroRNAs combined with the TLR4/TDAG8 mRNAs and proinflammatory cytokines are biomarkers for the rapid diagnosis of sepsis. Mol Med Rep 26: 334, 2022.
12. Zhou M, Li T, Lv S, Gan W, Zhang F, Che Y, Yang L, Hou Y, Yan Z, Zeng Z, *et al*: Identification of immune-related genes and small-molecule drugs in hypertension-induced left ventricular hypertrophy based on machine learning algorithms and molecular docking. Front Immunol 15: 1351945, 2024.
13. Daneshvar A and Mousa G: Regression shrinkage and selection via least quantile shrinkage and selection operator. PLoS One 18: e0266267, 2023.
14. Özer ME, Özbek Sarica P and Arğa KY: SVM-DO: Identification of tumor-discriminating mRNA signatures via support vector machines supported by disease ontology. Turk J Biol 47: 349-365, 2023.
15. Ignatenko V, Surkov A and Koltcov S: Random forests with parametric entropy-based information gains for classification and regression problems. PeerJ Comput Sci 10: e1775, 2024.
16. Long G and Yang C: A six-gene support vector machine classifier contributes to the diagnosis of pediatric septic shock. Mol Med Rep 21: 1561-1571, 2020.
17. Jiang Z, Luo Y, Wei L, Gu R, Zhang X, Zhou Y and Zhang S: Bioinformatic analysis and machine learning methods in neonatal sepsis: Identification of biomarkers and immune infiltration. Biomedicines 11: 1853, 2023.
18. Rangel-Frausto MS, Pittet D, Costigan M, Hwang T, Davis CS and Wenzel RP: The natural history of the systemic inflammatory response syndrome (SIRS). A prospective study. JAMA 273: 117-123, 1995.
19. Langfelder P and Horvath S: WGCNA: An R package for weighted correlation network analysis. BMC Bioinformatics 9: 559, 2008.

20. Ritchie ME, Phipson B, Wu D, Hu Y, Law CW, Shi W and Smyth GK: limma powers differential expression analyses for RNA-sequencing and microarray studies. Nucleic Acids Res 43: e47, 2015.
21. Wu T, Hu E, Xu S, Chen M, Guo P, Dai Z, Feng T, Zhou L, Tang W, Zhan L, *et al*: clusterProfiler 4.0: A universal enrichment tool for interpreting omics data. Innovation (Camb) 2: 100141, 2021.
22. Yu G, Wang LG, Yan GR and He QY: DOSE: an R/bioconductor package for disease ontology semantic and enrichment analysis. Bioinformatics 31: 608-609, 2015.
23. Hänzelmann S, Castelo R and Guinney J: GSVA: Gene set variation analysis for microarray and RNA-seq data. BMC Bioinformatics 14: 7, 2013.
24. Friedman J, Hastie T and Tibshirani R: Regularization paths for generalized linear models via coordinate descent. J Stat Softw 33: 1-22, 2010.
25. Tibshirani R, Bien J, Friedman J, Hastie T, Simon N, Taylor J and Tibshirani RJ: Strong rules for discarding predictors in lasso-type problems. J R Stat Soc Series B Stat Methodol 74: 245-266, 2012.
26. Wang Q and Liu X: Screening of feature genes in distinguishing different types of breast cancer using support vector machine. Onco Targets Ther 8: 2311-2317, 2015.
27. Alderden J, Pepper GA, Wilson A, Whitney JD, Richardson S, Butcher R, Jo Y and Cummins MR: Predicting pressure injury in critical care patients: A machine-learning model. Am J Crit Care 27: 461-468, 2018.
28. Wang H and Zhou L: Random survival forest with space extensions for censored data. Artif Intell Med 79: 52-61, 2017.
29. Tao X, Wang J, Liu B, Cheng P, Mu D, Du H and Niu B: Plasticity and crosstalk of mesenchymal stem cells and macrophages in immunomodulation in sepsis. Front Immunol 15: 1338744, 2024.
30. Wang Z and Wang Z: The role of macrophages polarization in sepsis-induced acute lung injury. Front Immunol 14: 1209438, 2023.
31. Han Y, Wang J, Zhang J, Zheng X, Jiang Y, Liu W and Li W: VX-702 ameliorates the severity of sepsis-associated acute kidney injury by downregulating inflammatory factors in macrophages. J Inflamm Res 17: 4037-4054, 2024.
32. Yu Y, Li Z, Liu C, Bu Y, Gong W, Luo J and Yue Z: Danlou tablet alleviates sepsis-induced acute lung and kidney injury by inhibiting the PARP1/HMGB1 pathway. Heliyon 10: e30172, 2024.
33. Chang BT, Wang Y, Tu WL, Zhang ZQ, Pu YF, Xie L, Yuan F, Gao Y, Xu N and Yao Q: Regulatory effects of mangiferin on LPS-induced inflammatory responses and intestinal flora imbalance during sepsis. Food Sci Nutr 12: 2068-2080, 2023.
34. Lund ME, To J, O'Brien BA and Donnelly S: The choice of phorbol 12-myristate 13-acetate differentiation protocol influences the response of THP-1 macrophages to a pro-inflammatory stimulus. J Immunol Methods 430: 64-70, 2016.
35. Zhang S, Guan X, Liu W, Zhu Z, Jin H, Zhu Y, Chen Y, Zhang M, Xu C, Tang X, *et al*: YTHDF1 alleviates sepsis by upregulating WWP1 to induce NLRP3 ubiquitination and inhibit caspase-1-dependent pyroptosis. Cell Death Discov 8: 244, 2022.
36. Livak KJ and Schmittgen TD: Analysis of relative gene expression data using real-time quantitative PCR and the 2(-Delta Delta C(T)) method. Methods 25: 402-408, 2001.
37. Yan L, Chen C, Wang L, Hong H, Wu C, Huang J, Jiang J, Chen J, Xu G and Cui Z: Analysis of gene expression in microglial apoptotic cell clearance following spinal cord injury based on machine learning algorithms. Exp Ther Med 28: 292, 2024.
38. Wysocki K, Conley Y and Wenzel S: Epigenome variation in severe asthma. Biol Res Nurs 17: 263-269, 2015.
39. Kumari R, Kumar S, Thakur VK, Singh K and Kumar U: MTHFR C677T and MTR A2756G gene polymorphism in neural tube defect patients and its association with red blood cell folate level in Eastern Indian population. J Indian Assoc Pediatr Surg 27: 699-706, 2022.
40. Jing HW, Yin L, Yu HY, Zuo L and Liu T: MTR D919G variant is associated with prostate adenocarcinoma risk: Evidence based on 51106 subjects. Eur Rev Med Pharmacol Sci 24: 8329-8340, 2020.
41. Nitsch L, Ehrentraut SF, Grobe-Einsler M, Bode FJ, Banat M, Schneider M, Lehmann F, Zimmermann J and Weller J: The diagnostic value of cerebrospinal fluid lactate for detection of sepsis in community-acquired bacterial meningitis. Diagnostics (Basel) 13: 1313, 2023.
42. Gao H, Ren Y and Liu C: Aloe-emodin suppresses oxidative stress and inflammation via a PI3K-dependent mechanism in a murine model of sepsis. Evid Based Complement Alternat Med 2022: 9697887, 2022.
43. Gao N, Tang AL, Liu XY, Chen J and Zhang GQ: p53-Dependent ferroptosis pathways in sepsis. Int Immunopharmacol 118: 110083, 2023.
44. Bai X, He T, Liu Y, Zhang J, Li X, Shi J, Wang K, Han F, Zhang W, Zhang Y, *et al*: Acetylation-dependent regulation of notch signaling in macrophages by SIRT1 affects sepsis development. Front Immunol 9: 762, 2018.
45. Chou KT, Cheng SC, Huang SF, Perng DW, Chang SC, Chen YM, Hsu HS and Hung SC: Impact of intermittent hypoxia on sepsis outcomes in a murine model. Sci Rep 9: 12900, 2019.
46. Ding W, Huang L, Wu Y, Su J, He L, Tang Z and Zhang M: The role of pyroptosis-related genes in the diagnosis and subclassification of sepsis. PLoS One 18: e0293537, 2023.
47. Wang Y, Fan Y, Jiang Y, Wang E, Song Y, Chen H, Xu F, Xie K and Yu Y: APOA2: New target for molecular hydrogen therapy in sepsis-related lung injury based on proteomic and genomic analysis. Int J Mol Sci 24: 11325, 2023.
48. Dai W, Zheng P, Luo D, Xie Q, Liu F, Shao Q, Zhao N and Qian K: LPIN1 is a regulatory factor associated with immune response and inflammation in sepsis. Front Immunol 13: 820164, 2022.
49. Sánchez-Baizán N, Ribas L and Piferrer F: Improved biomarker discovery through a plot twist in transcriptomic data analysis. BMC Biol 20: 208, 2022.
50. Alhamzawi R and Ali HTM: The Bayesian adaptive lasso regression. Math Biosci 303: 75-82, 2018.
51. Chen H, Chen E, Lu Y and Xu Y: Identification of immune-related genes in diagnosing retinopathy of prematurity with sepsis through bioinformatics analysis and machine learning. Front Genet 14: 1264873, 2023.
52. Yu J, Wu X, Huang K, Zhu M, Zhang X, Zhang Y, Chen S, Xu X and Zhang Q: Bioinformatics identification of lncRNA biomarkers associated with the progression of esophageal squamous cell carcinoma. Mol Med Rep 19: 5309-5320, 2019.
53. Chicco D and Jurman G: The advantages of the Matthews correlation coefficient (MCC) over F1 score and accuracy in binary classification evaluation. BMC Genomics 21: 6, 2020.
54. Safránek R, Holecek M, Sispera L and Muthný T: Aspects of protein and amino acid metabolism in a model of severe glutamine deficiency in sepsis. Ann Nutr Metab 50: 361-367, 2006.
55. Laufenberg LJ, Pruznak AM, Navaratnarajah M and Lang CH: Sepsis-induced changes in amino acid transporters and leucine signaling via mTOR in skeletal muscle. Amino Acids 46: 2787-2798, 2014.
56. Zhang J, Ding N, He Y, Tao C, Liang Z, Xin W, Zhang Q and Wang F: Bioinformatic identification of genomic instability-associated lncRNAs signatures for improving the clinical outcome of cervical cancer by a prognostic model. Sci Rep 11: 20929, 2021.
57. Pokushalov E, Ponomarenko A, Bayramova S, Garcia C, Pak I, Shrainer E, Ermolaeva M, Kudlay D, Johnson M and Miller R: Effect of methylfolate, pyridoxal-5'-phosphate, and methylcobalamin (Soloways™) supplementation on homocysteine and low-density lipoprotein cholesterol levels in patients with methylenetetrahydrofolate reductase, methionine synthase, and methionine synthase reductase polymorphisms: A randomized controlled trial. Nutrients 16: 1550, 2024.
58. Chen J, Tang S, Ke S, Cai JJ, Osorio D, Golovko A, Morpurgo B, Guo S, Sun Y, Winkle M, *et al*: Ablation of long noncoding RNA MALAT1 activates antioxidant pathway and alleviates sepsis in mice. Redox Biol 54: 102377, 2022.
59. Ping F, Li Y, Cao Y, Shang J, Zhang Z, Yuan Z, Wang W and Guo Y: Metabolomics analysis of the development of sepsis and potential biomarkers of sepsis-induced acute kidney injury. Oxid Med Cell Longev 2021: 6628847, 2021.
60. Yoo HJ, Choi DW, Roh YJ, Lee YM, Lim JH, Eo S, Lee HJ, Kim NY, Kim S, Cho S, *et al*: MsrB1-regulated GAPDH oxidation plays programmatic roles in shaping metabolic and inflammatory signatures during macrophage activation. Cell Rep 41: 111598, 2022.
61. Bi CF, Liu J, Hao SW, Xu ZX, Ma X, Kang XF, Yang LS and Zhang JF: Xuebijing injection protects against sepsis-induced myocardial injury by regulating apoptosis and autophagy via mediation of PI3K/AKT/mTOR signaling pathway in rats. Aging (Albany NY) 15: 4374-4390, 2023.

62. Geng H, Zhang H, Cheng L and Dong S: Sivelestat ameliorates sepsis-induced myocardial dysfunction by activating the PI3K/AKT/mTOR signaling pathway. Int Immunopharmacol 128: 111466, 2024.
63. Manning BD and Cantley LC: AKT/PKB signaling: Navigating downstream. Cell 129: 1261-1274, 2007.
64. Jiang L, Yang D, Zhang Z, Xu L, Jiang Q, Tong Y and Zheng L: Elucidating the role of Rhodiola rosea L. in sepsis-induced acute lung injury via network pharmacology: Emphasis on inflammatory response, oxidative stress, and the PI3K-AKT pathway. Pharm Biol 62: 272-284, 2024.
65. Wang Y, Wang D, Dai Y, Kong X, Zhu X, Fan Y, Wang Y, Wu H, Jin J, Yao W, *et al*: Positive crosstalk between hedgehog and NF-κB pathways is dependent on KRAS mutation in pancreatic ductal adenocarcinoma. Front Oncol 11: 652283, 2021.
66. Ibrahim MA, Khalifa AM, Abd El-Fadeal NM, Abdel-Karim RI, Elsharawy AF, Ellawindy A, Galal HM, Nadwa EH, Abdel-Shafee MA and Galhom RA: Alleviation of doxorubicin-induced cardiotoxicity in rat by mesenchymal stem cells and olive leaf extract via MAPK/TNF-α pathway: Preclinical, experimental and bioinformatics enrichment study. Tissue Cell 85: 102239, 2023.
67. Tokumaru Y, Oshi M, Katsuta E, Yan L, Satyananda V, Matsuhashi N, Futamura M, Akao Y, Yoshida K and Takabe K: KRAS signaling enriched triple negative breast cancer is associated with favorable tumor immune microenvironment and better survival. Am J Cancer Res 10: 897-907, 2020.
68. Xu M, Feng Y, Xiang X, Liu L and Tang G: MZB1 regulates cellular proliferation, mitochondrial dysfunction, and inflammation and targets the PI3K-Akt signaling pathway in acute pancreatitis. Cell Signal 118: 111143, 2024.
69. Singh SP, Dosch AR, Mehra S, De Castro Silva I, Bianchi A, Garrido VT, Zhou Z, Adams A, Amirian H, Box EW, *et al*: Tumor cell-intrinsic p38 MAPK signaling promotes IL1α-mediated stromal inflammation and therapeutic resistance in pancreatic cancer. Cancer Res 84: 1320-1332, 2024.
70. Mo JS, Lamichhane S, Yun KJ and Chae SC: MicroRNA 452 regulates SHC1 expression in human colorectal cancer and colitis. Genes Genomics 45: 1295-1304, 2023.
71. Li J, Xu F, Li S, Xie M and Li N: Gentamicin promoted the production of $CD4^+CD25^+$ Tregs via the STAT5 signaling pathway in mice sepsis. BMC Immunol 23: 47, 2022.
72. Ge Y, Huang M, Wu Y, Dong N and Yao YM: Interleukin-38 protects against sepsis by augmenting immunosuppressive activity of $CD4^+$ $CD25^+$ regulatory T cells. J Cell Mol Med 24: 2027-2039, 2020.
73. Li F, Xia Y, Yuan S, Xie X, Li L, Luo Y, Du Q, Yuan Y and He R: α-Aminobutyric acid constrains macrophage-associated inflammatory diseases through metabolic reprogramming and epigenetic modification. Int J Mol Sci 24: 10444, 2023.
74. Zhang Y, Yu W, Han D, Meng J, Wang H and Cao G: L-lysine ameliorates sepsis-induced acute lung injury in a lipopolysaccharide-induced mouse model. Biomed Pharmacother 118: 109307, 2019.
75. Hou YC, Wu JM, Chen KY, Chen PD, Lei CS, Yeh SL and Lin MT: Effects of prophylactic administration of glutamine on $CD4^+$ T cell polarisation and kidney injury in mice with polymicrobial sepsis. Br J Nutr 122: 657-665, 2019.
76. Steinacher E, Lenz M, Krychtiuk KA, Hengstenberg C, Huber K, Wojta J, Heinz G, Niessner A, Speidl WS and Koller L: Decreased percentages of plasmacytoid dendritic cells predict survival in critically ill patients. J Leukoc Biol 115: 902-912, 2024.
77. Bi Q, Liu Y, Yuan T, Wang H, Li B, Jiang Y, Mo X, Lei Y, Xiao Y, Dong S, *et al*: Predicted $CD4^+$ T cell infiltration levels could indicate better overall survival in sarcoma patients. J Int Med Res 49: 300060520981539, 2021.
78. Zhu W, Ou Y, Wang C, An R, Lai J, Shen Y, Ye X and Wang H: A neutrophil elastase inhibitor, sivelestat, attenuates sepsis-induced acute kidney injury by inhibiting oxidative stress. Heliyon 10: e29366, 2024.
79. Bacârea A, Coman O, Bacârea VC, Văsieşiu AM, Săplăcan I, Fodor RŞ and Grigorescu BL: Immune profile of patients-a new approach in management of sepsis and septic shock? Exp Ther Med 27: 203, 2024.
80. Zhang S, Liu Y, Zhang XL, Sun Y and Lu ZH: ANKRD22 aggravates sepsis-induced ARDS and promotes pulmonary M1 macrophage polarization. J Transl Autoimmun 8: 100228, 2023.
81. Weckbecker M, Anžel A, Yang Z and Hattab G: Interpretable molecular encodings and representations for machine learning tasks. Comput Struct Biotechnol J 23: 2326-2336, 2024.